Applications of Centrifuge Modelling to Liquefaction Mitigation Techniques

M. Kitazume
Tokyo Institute of Technology, Tokyo, Japan

ABSTRACT: Many earthquakes take place every year in Japan, in which the 1995 Hyogoken-Nambu earthquake and the 2011 Tōhoku earthquake induced both a humanitarian crisis and massive economic impacts. As liquefaction which occur in a loose and saturated sand layer, induces quite large damages of infrastructures, the importance of liquefaction mitigation has been emphasized to minimize earthquake disasters for many years. Many kinds of ground improvement techniques based on various improvement principles have been developed for liquefaction mitigation. Among them, the grid type deep mixing method was developed for liquefaction mitigation in the 1990s, where the grid of stabilized column walls function to restrict generation of excess pore pressure by confining the soil particle movement during earthquake. The improvement effect of the method was first evaluated in the Hyogoken-Nambu earthquake in 1995. A simple design guideline was established based on the experimental and numerical studies, and modified to achieve high applicability and reliability. Many centrifuge model tests were conducted to investigate the effect of grid wall space on the generation of pore pressure and to brush up the design guideline. The manuscript briefly introduces the applications and contributions of the centrifuge model testing to develop the new type of liquefaction mitigation technique and design procedure.

1 INTRODUCTION

It is an obvious truism that, structures should be constructed on a stiff and stable ground. The ground conditions of construction sites, however, have become worse than ever during recent decades throughout the world. Soft cohesive ground is often encountered at many infrastructure constructions, in which large ground settlement and stability failure are anticipated. Apart from cohesive soil grounds, loose sand deposit under a water table can cause serious problem of liquefaction under seismic condition. Liquefaction has been thoroughly brought to the attention of engineers since the 1964 Niigata earthquake and the 1964 Alaska earthquake. Liquefaction was a major factor in the destruction and damages in many earthquakes such as the 1989 Loma Prieta earthquake, the 1995 Hyogoken-Nambu earthquake, the 2010 Canterbury earthquake, the 2011 Christchurch earthquakes and the 2011 Tōhoku earthquake. In fact, port and harbor facilities at Kobe Port were heavily damaged by liquefaction in the 1995 Hyogoken-Nambu earthquake, where gravity type of sea revetments displaced a couple of meters toward sea together with large ground settlement at backfill yard, as later shown in Figure 14. Table 1 tabulates the amount of damage to port facilities caused by

Table 1 Comparison of amount of damage (Noda, 1991).

Earth-quake	Magnitude	Port	Soil type	Max. accel. (*gal*)	Liquefaction	Damage (million yen)
Niigata, 1964	7.9	Hachiohe	Sand	233	No	1,980*
Tokachi Oki, 1968	7.5	Niigata	Sand	159	yes	49,700*
Miyagiken Oki, 1978	7.4	Shiogama	Clay	273	No	160*
	7.4	Ishinomaki	Sand	195-210	Yes	3,008*
Urakawa Oki, 1982	7.3	Muroran	Sand	164	No	120
Nihonkai Chubu, 1983	7.7	Akita	Sand	205	Yes	6,400

* converted into 1978 prices.

strong earthquakes (Noda, 1991), and demonstrates quite large difference in the damage depending on whether liquefaction took place or not. According to the table, the amount of damage when liquefaction took place was about 20 to 50 times larger than that when liquefaction didn't take place. This highlights the importance of liquefaction mitigation to minimize earthquake disasters.

Many types of ground improvement techniques were developed to prevent liquefaction and reinforce seismic performance of ground; such as gravel drain method, sand compaction pile method and deep mixing method. Many numerical analyses, physical model tests and field tests have been conducted to investigate the interaction of the improved ground and the surrounding ground and the performance of ground improvement (*e.g.* Kitazume, 2009). Based on these researches together with observations and experiences in the fields, design procedures and execution and quality control and assurance for each ground improvement technique have been established and brushed up (*e.g.* Ministry of Land, Infrastructure, Transport & Tourism. 2007).

The behavior of improved ground is affected by many factors such as the properties of original ground and improved ground, the interaction between original and improved grounds, and the external loading conditions, *etc*. Among many ground improvement techniques, the grid type deep mixing method has been often applied to liquefaction mitigation. In the method, the stiff grid walls are constructed by mixing the soil and binder in-situ, which are expected to restrict the shear deformation of the soil within the grid walls so that the pore water pressure generation can be remained small. The method was developed more than 20 years ago and its high applicability was confirmed in several earthquakes; the 1995 Hyogoken-Nambu earthquake and the 2011 Tōhoku earthquake. In order to establish and brush up the design procedure of the method, many centrifuge model tests, large scale shaking table tests and numerical analyses have been carried out. In this manuscript, some of the centrifuge model tests are exemplified to discuss their applications to develop and brush up the grid type deep mixing method for liquefaction mitigation.

2 DEEP MIXING METHOD

2.1 *Outline of the method*

The Deep Mixing Method (DMM), an in-situ admixture stabilization technique using cement and/or lime as a binder, has been applied in many construction projects for various improvement purposes (Kitazume and Terashi, 2013). The DMM was developed and put into practice in Japan in the middle of 1970s to improve soft marine deposits to assure the stability of structure and reduce the ground settlement in on land and marine constructions. Similar technique was developed in Sweden in the 1970s, in which quicklime was used as a binder to construct stabilized soil columns with low strength mainly for reducing ground settlement.

Four decades of practice have made equipment improved, binders changed, and applications diversified, which were presented in the series of the deep mixing conferences. Lime was replaced by cement in Japan. Figure 1(a) and 1(b) show Japanese DM machines for on land and marine constructions. The special machine used to stabilize soft soil is basically composed of several mixing shafts and blades, a binder-supplying system and a control system.

(a) for on land construction

(b) for marine construction

Figure 1. Deep mixing machines.

2.2 *Installation patterns of DM improved ground*

In one operation, a column of stabilized soil is constructed in a ground. Through a series of construction steps, any arbitrary shape of improved ground can be constructed in a ground; block, grid, wall and group column types as shown in Figure 2 (Kitazume and Terashi, 2013).

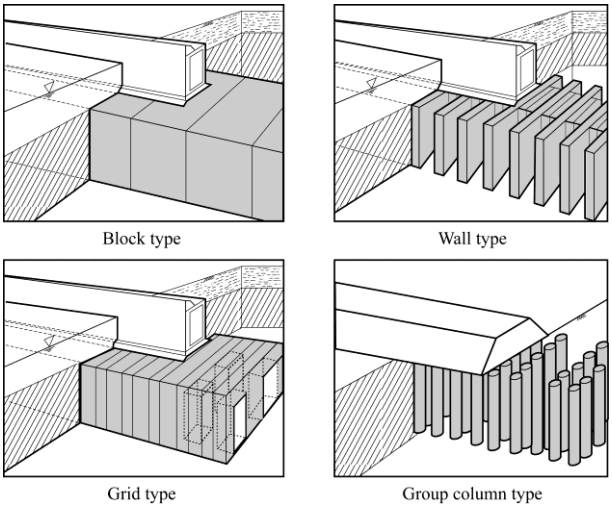

Figure 2. Installation patterns of deep mixing improved ground.

The block, grid and wall types are manufactured by overlapping deep-mixed stabilized soil columns or elements. The block type is the most stable against both the external and internal stabilities among all the patterns. It may find application in case of breakwater or large scale earth retaining structure which is subjected to large horizontal forces. The grid type has almost the same function as the block type with less stabilized soil volume, which can be applicable when the internal stability is less critical compared to block (Kazama *et al*., 1983). When the internal stability is dominant to one direction, the wall type can effectively improve the stability. The grid type and the wall type installation patterns may be selected in order to assure the stability of embankment slope or foundation support for retaining structure. When the major concern is the consolidation settlement of soft ground under an embankment or a light weight structure, group column type can provide a good solution. The tangent group column is a modified improvement pattern of the group column type improvement, where stabilized soil columns are installed in contact with the adjacent columns without overlapping. This improvement has frequently applied to embankment slope and small building for increasing stability and bearing capacity respectively.

2.3 *Application to earthquake disaster mitigation*

As explained above, the DMM was originally developed for stabilize cohesive soils and organic soils to assure stability of structure and to reduce ground settlement. Since the high strength of stabilized soil can be obtained within a short term, the block and grid type deep mixing improvements have been also applied to liquefaction prevention. In the block type improvement, a whole area of liquefiable soil is stabilized in order to increase liquefaction resistance.

Figures 3 shows an example of the block type application at No. 2 Pier at Kushiro Port (Yamazaki, 2000). The reclaimed layers up to the depth of -8.0 m consisted of several sand layers whose SPT *N*-value was quite small. In 1993, the pier was subjected to the large earthquake of Magnitude of 7.9 (Kushiro Oki Earthquake) and heavily damaged by liquefaction in the reclaimed layers (Inatomi *et al*., 1997). Displacements of the concrete caisson of 0.20 to 0.305 m in horizontal and 0.30 to 0.15 m in vertical were reported. After the earthquake, the reclaimed sand layers were improved by the deep mixing and the gravel drain method, both for liquefaction mitigation, as shown in Figure 3(a). The design field unconfined compressive strength, q_u was as small as 100 kN/m^2, which was sufficient to increase liquefaction resistance of the sand (Zen *et al*., 1987).

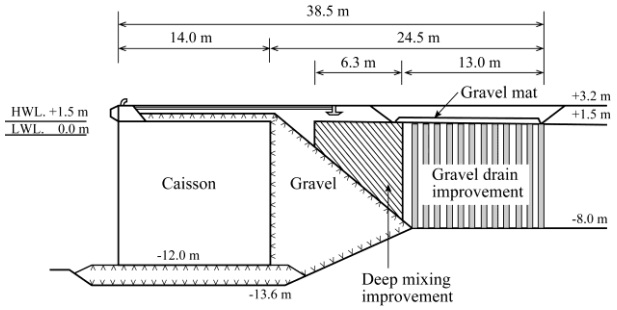

(a) Application of DMM at Kushiro Port.

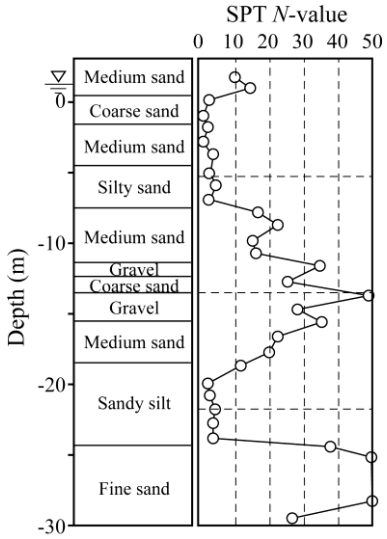

(b) Ground profile at No. 2 Pier at Kushiro Port.

Figure 3 Application of block type improvement at Kushiro Port (Yamazaki, 2000).

The pier was again subjected to the Hokkaido Toho-Oki earthquake of Magnitude of 8.5 later in 1994. Figure 4 shows the performance of unimproved and improved areas respectively (Yamazaki, 2000). Figure 4(a) shows heavy damages and many cracks of pavement behind the pier at unimproved area, which was caused by the liquefaction. However, due to the ground improvement, negligible damage took place at the improved area as shown in Figure

4(b), which has revealed the high applicability of deep mixing method for liquefaction mitigation and reinforcement of sea revetment.

(a) Unimproved area.

(b) Improved area.

Figure 4. Performance of improved area in Hokkaido Toho-Oki Earthquake (Yamazaki, 2000).

3. DEVELOPMENT OF GRID TYPE IMPROVEMENT

3.1 *Centrifuge model test on effect of grid space*

Many centrifuge model testing have been often applied to investigate the liquefaction mechanism and the effects of various ground improvement techniques. Some of them were presented in the several Centrifuge Conferences. However, the number of centrifuge tests on the grid type deep mixing method is limited. The development of the grid type of improved ground for liquefaction mitigation was initiated by the Ministry of Construction in the late 1980s by a collaborative study with several Japanese construction firms. In the grid type improvement, the grid walls with high strength and stiffness are expected to restrict the shear deformation of soil between the walls during earthquake. The spacing of the grid wall is one of the essential factors for the liquefaction design, which the thickness and strength of the grid wall are the other essential factors for the external and internal stabilities. In the collaborative study, centrifuge model tests, large scale shaking table test and numerical analyses were carried out to investigate these factors (Suzuki *et al*., 1990; Babasaki *et al*., 1991; Koga *et al*., 1986, 1988; Koseki *et al*., 1991; Matsuo *et al*., 1991a, 1991b; Matsuo and Shimizu, 1994).

Here, one of the centrifuge model tests on the former factor is briefly introduced. A series of centrifuge model test was carried out by the University of Chuo 3.05 m radius centrifuge (Fujii *et al*., 1988) to investigate the effect of grid spacing on liquefaction prevention (Suzuki *et al*., 1991; Babasaki *et al*., 1992). In the tests, the model ground was prepared in a laminar box, which consisted of loose Toyoura sand (*Dr* of 52%) with 10 cm in thickness and the dry fine aggregate of concrete material as a bearing stratum, as shown in Figure 5 (Suzuki *et al*., 1991). The grid shape ground was fabricated by light-weight precast concrete. The inside dimensions of each grid were 5.0, 7.5, 10.0, 12.5 and 18.8 cm. After saturating the model ground and the baring stratum with glycerin solution, the model ground was subjected to several seismic loadings under 100 *G* centrifuge field.

Figure 6 shows the summary of the test on the effect of grid space on the pore water generation. Figure 6(a) shows the relationship between the pore water ratio, $\Delta u/\sigma_v'$ and *L*/*H* ratio in the case of the water table is equal to the ground surface, where *L* and *H* are the grid space and thickness of the loose sand layer. It can be found that the pore water pressure ratio at 2 cm depth increase close to 1.0 in the case of the *L*/*H* exceeding about 1.0, which indicates liquefaction takes place. In the case of the *L*/*H* is 0.5, the $\Delta u/\sigma_v'$ remains small value of about 0.3. Similar test results is shown in Figure 6(b) for the case of the water table is 1.0 cm below the ground surface. The increase in the overburden pressure by water table

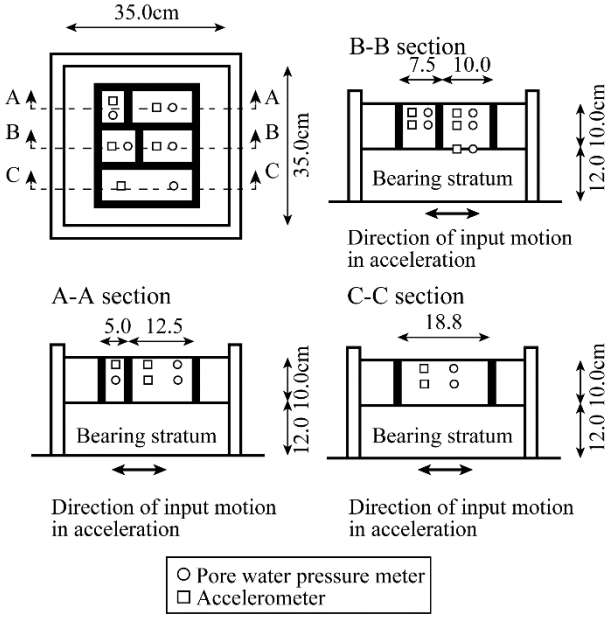

Figure 5. Improved model ground (Suzuki *et al*., 1991).

decrease could function to decrease the $\Delta u/\sigma_v'$ increase, where no liquefaction took place even in the case of the *L*/*H* exceeding 1.0. The test results have clearly shown the high applicability of the grid type deep mixing method for liquefaction prevention and the ratio of the grid space and the thickness of loose sand layer, *L*/*H* was one of the critical parameters for liquefaction mitigation.

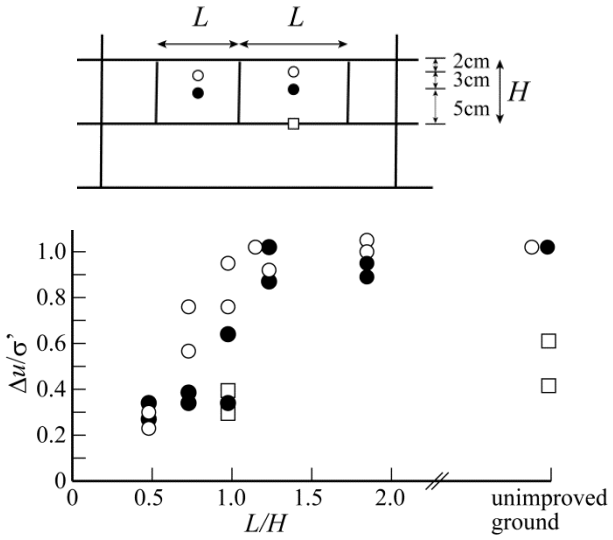

(a) Ground water level, G.L. 0.0 cm.

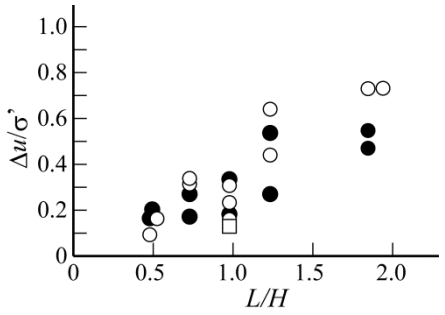

(b) Ground water level, G.L. -1.0 cm.

Figure 6. Relationship between maximum excess pore water pressure ratio and *L*/*H* (Babasaki *et al*., 1992).

3.2 *Large scale shaking table test for stability*

On the later research topics on the external and internal stabilities, Matsuo *et al*. (1996) carried out large scale shaking table tests. Figure 7 illustrates the model ground, which consists of an improved body (grid wall) and a liquefiable sandy stratum (loose sandy layer). The improved body of 80 cm in width, 68 cm in length and 40 cm in height was manufactured by dry-mixed mortar, whose shear strength was controlled 12.3 kN/m^2. In the body, six grids of 16 cm in width, 24 cm in length and 40 cm in height were consisted as shown in Figure 7(b). The model ground was subjected to the seismic loading of the sinusoidal wave of the frequency of 5 Hz and 20 cycles. The seismic load was increased in stages to cause the failure of the grid wall.

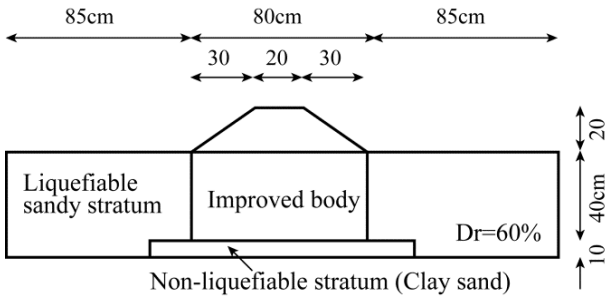

(a) Front view.

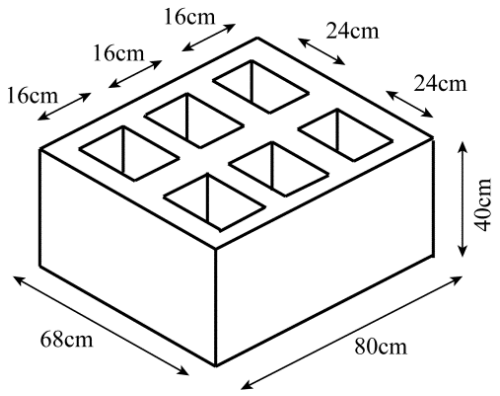

(b) Shape of improved body.

Figure 7. Testing model for shaking table test (Matsuo *et al*., 1996).

Figure 8(a) shows the accumulated settlement of the embankment along the seismic loading. In the figure, the measured ground settlement of the unimproved ground is also plotted for comparison (Washida *et al*., 1993). In the case of the unimproved ground, the embankment settled substantially at the seismic loading of 150 *gal*. After then, the ground settlement increased with the further seismic loadings. In the case of the improved ground, on the other hand, negligible settlement took place as far as the seismic loading of 200 *gal*, after then the ground settlement increased with the further seismic loadings, but the magnitude of the ground settlement was smaller than that of the unimproved ground. Figure 8(b) shows the ground deformation of the improved ground after the seismic loading of 400 *gal*, where the top of the embankment settled about 3.5 cm and the ground close to the grid wall spread horizontally about 0.9 to 1.1 cm. Based on the test results, it could be estimated that the stabilized grid wall failed at the loading with around 200 to 250 *gal*. Figure 8(c) shows the observed failure of the grid wall after reassembling the model ground, where many vertical tensile cracks were found in the wall pane, and several part of the wall were chipped off at the toe of the wall perpendicular to the loading direction. These test results suggested that the stabilized grid wall was failure with the vertical shear force and with compressive stress at the toe of the wall. But they didn't find which failure mode took first.

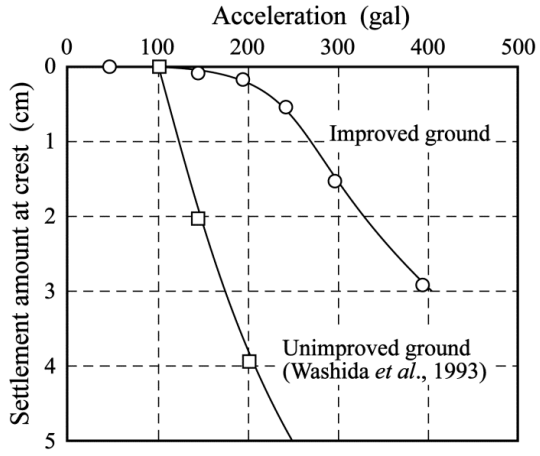

(a) Measured settlement at crest.

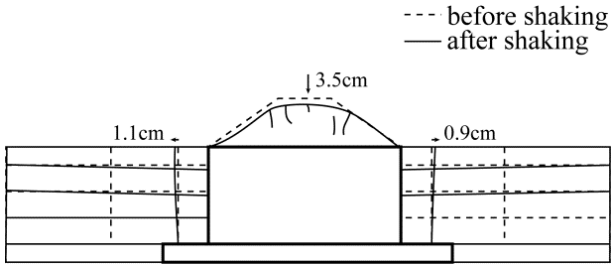

(b) Deformation of model after shaking at 400 *gal*.

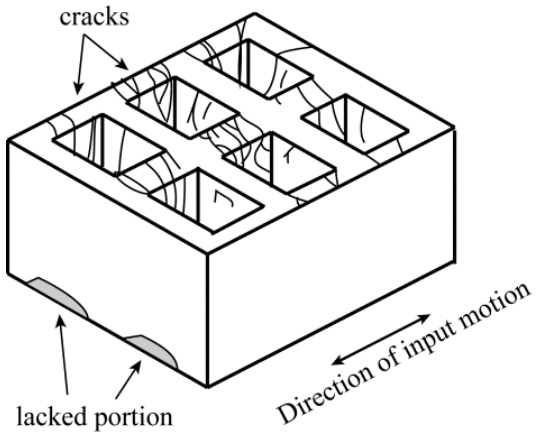

(c) Failure in improved body.

Figure 8. Deformation and failure of model ground (Matsuo *et al*., 1996).

3.3 *Design procedure of grid type deep mixing method*

According to the centrifuge and large scale shaking table tests together with the numerical analyses (Koseki *et al*., 1991), the Ministry of Construction proposed the draft of the design procedure and guideline of the grid type deep mixing improvement in 1999 (Ministry of Construction, 1999). Figure 9 shows the design flow of the grid type improvement, which consists of the assumption of dimension of improved ground (examination of grid space for liquefaction mitigation), examinations of external stability and internal stability, and slip circle analysis.

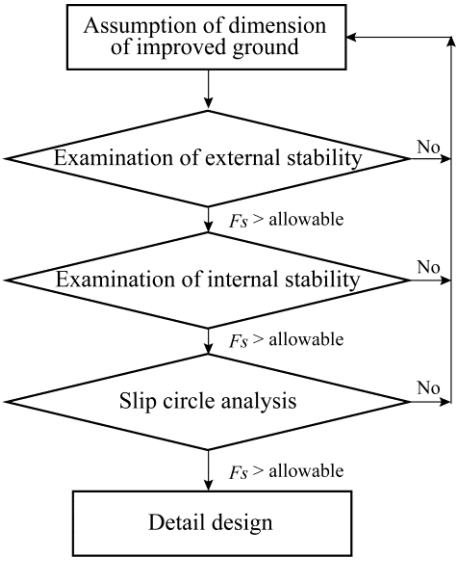

Figure 9. Design flow of grid type deep mixing method (Ministry of Construction, 1999).

In the assumption of dimension of improved ground, the ratio of the grid space and thickness of liquefiable layer, *L/H* is determined by Figure 10 at first. In the figure, the maximum excess pore pressure ratio, $\Delta u/\Delta\sigma_v'$ at the mid depth of potentially liquefiable layer is plotted. The Ministry recommended that the grid ratio, B_{cl}/H_i (same as *L/H*) should be smaller than about 0.8 to assure the effect of liquefaction prevention. As the fixed type improved ground, where the grid walls reach a bottom stiff layer) is desirable from the view point of stability and displacement, the thickness of potentially liquefiable layer is assumed to be the full thickness of soft layer, H_c.

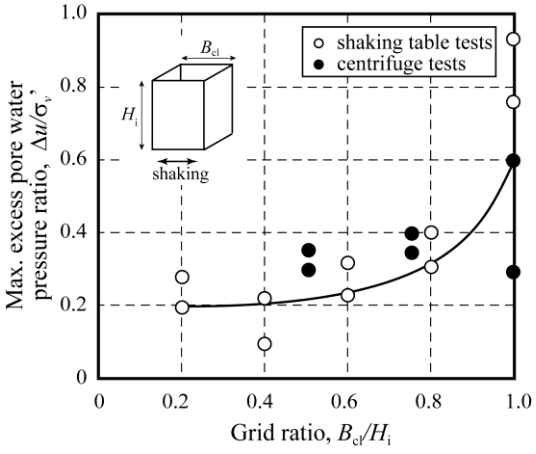

Figure 10. Design flow of grid type improvement for liquefaction prevention (Ministry of Construction, 1999).

In the external stability analysis of the improved ground, three failure modes are examined: sliding, overturning and bearing capacity failures. In the examination of sliding failure, it is assumed that the improved ground moves horizontally by the active

earth pressure due to the embankment and the seismic inertia force of the improved ground. The sliding and overturning stabilities are calculated by the equilibrium of horizontal and moment forces.

In the internal stability analysis, the induced stresses due to the weight of structure and seismic inertia loads in the improved ground are calculated based on the elastic theory. The width of improved ground and the thickness of grid wall are determined so that the induced stresses become lower than the allowable strengths of the stabilized soil. In the calculation, the stabilized soil is generally assumed to have uniform property for the sake of simplicity even it contains possibly weaker zones due to construction process such as overlap joints.

In the slip circle analysis, the overall stability of the improved ground, structure and soft ground is evaluated. As the strength of stabilized soil is usually very high value, a slip circle analysis passing through the improved ground is not necessary in many cases. The safety factor against the slip circle failure is usually calculated by the modified Fellenius analysis.

3.4 *Application of the grid type DMM*

The grid type of DM improved ground was designed based on the design procedure described in the previous section and applied to a building foundation at Kobe port to prevent excess pore water pressure generation during earthquake. Figure 11 shows the 14-story building located on Meriken Wharf in Kobe.

Figure 11. A 14 –story building on the grid type deep mixing method.

Figure 12 shows the soil profile at the site which consisted of 10 to 12 m of soft reclaimed sand and gravel layers over the seabed (Tokimatsu *et al*., 1996; Suzuki *et al*., 1996). The seabed soil consisted of alternating layers of clay, sand and gravel. As small SPT *N*-value lower than 10, the top layer had been anticipated to liquefy due to earthquake excitation. The building was supported by cast-in-place reinforced concrete piles with a diameter of 2.5 m extending to dense diluvial sand and gravel at a depth of 33 m. Its section and plan diagrams are shown in Figure 13 (Suzuki *et al*., 1996). A grid type improvement was applied to prevent liquefaction in the upper loose fill. More than 1,000 stabilized soil columns with a diameter of 1.0 m were constructed where 200 kg/m^3 of blast furnace slag cement type B was mixed to obtain 2,400 kN/m^2 in q_u for the sand layer and 3,600 kN/m^2 for the clay layer. The improvement area ratio was approximately 0.2. The unconfined compressive strength of the stabilized soil after about six weeks curing was 4 to 6 MN/m^2 (Suzuki *et al*., 1996).

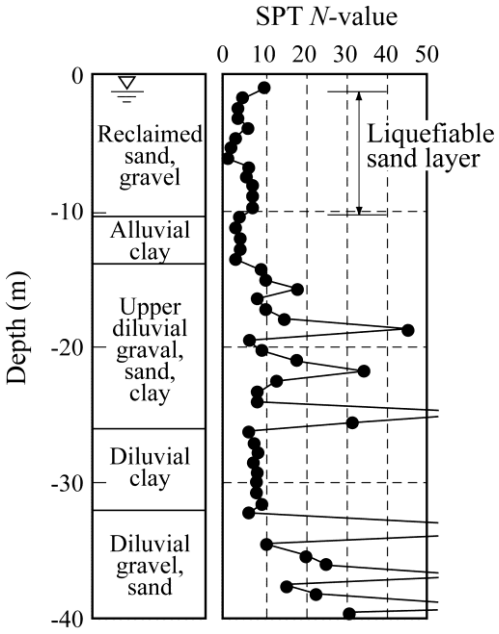

Figure 12. Ground condition at Kobe Port (Tokimatsu *et al*., 1996; Suzuki *et al*., 1996).

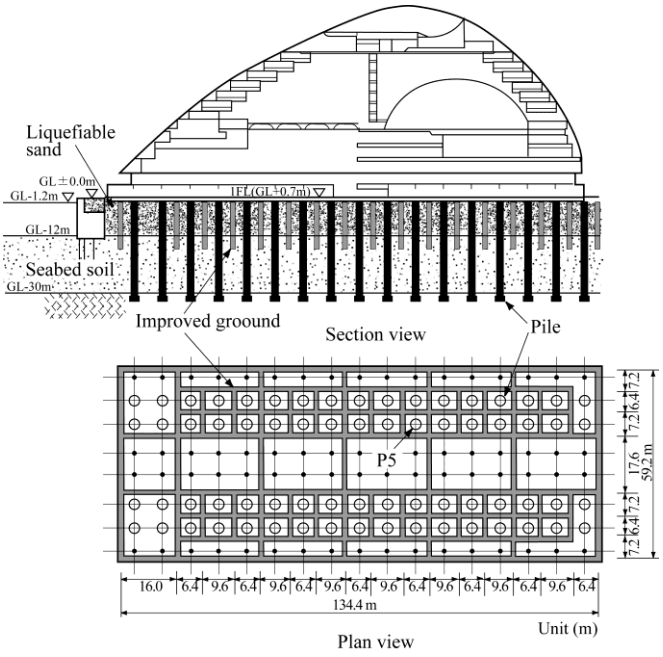

Figure 13. Grid type improved ground (Suzuki *et al*., 1996).

During the construction, the building and the improved ground were subjected to the large earthquake in 1995. As the reclaimed ground around the building was not improved, liquefaction took place during the

earthquake. Figure 14(a) shows the damage of quay wall near the building after the earthquake. The concrete caisson type quay walls were subjected to the large excess pore water pressure due to the liquefaction, and they on the west, south and east displaced horizontally towards the sea by 1 m, 2 m, and 0.6 m respectively and the ground behind the quay walls settled by 0.5 m, 0.6 m and 0.3 m. Sand boils and ground cracks were observed at the ground surface outside of the building. In the building, however, there was no crack at the surface of the improved ground as shown in Figure 14(b). The head of the cast-in-place piles supporting the building was found to be intact. Moreover, negligible differential settlement was observed on the first floor of the building. They have indicated that the grid type improvement to restrain the shear deformation of loose sand could mitigate the liquefaction damage to pile foundation and superstructure.

The three-dimensional FEM analyses were performed to investigate the behavior of the grid type deep mixing improved ground and the effect of the dimensions and strength of the grid walls (Namikawa et al., 2005, 2007). The analytical results suggested that the increase in the improvement area ratio is particularly effective in increasing the potential of the improved ground for liquefaction mitigation.

(a) Damage of sea revetment near the building.

(b) Parking area in the building.

Figure 14. Ground deformation after Kobe earthquake.

4. MODIFICATION OF THE DESIGN OF GRID TYPE IMPROVEMENT

4.1 *Centrifuge test on effect of grid space*

The success application of the grid type deep mixing to liquefaction prevention in the 1995 Hyogoken-Nambu earthquake has revealed the high applicability of the design procedure and guideline (Figures 9 and 10). However, the design procedure, didn't take into account the different seismic behavior at different depths but evaluates the possibility of liquefaction only at the mid-depth. In addition, the guideline contains an unreasonable issue, where the size of grid should be small as the thickness of liquefiable sand layer becomes small. In order to investigate the effect of grid space and brush up the design guideline, several centrifuge and numerical simulations were carried out.

The research group of the Port and Airport Research Institute carried out a series of centrifuge model tests to investigate the effect of grid spacing on generation of pore pressure and seismic response in a sand layer (Takahashi and Hayano, 2006; Takahashi *et al.*, 2006). An example of model grounds is schematically shown in Figure 15(a), where two model grounds with different sizes were prepared in a specimen box for conducting many tests. The model grid with the height, H, of 14 cm was made of Bakelite panels with the thickness of 2 cm, as shown in Figure 15(b). The model grid was fixed on the specimen box with bolts. Several model grids were prepared to perform parametric tests.

The sand material used in the study was Soma sand, whose U_c and D_{10} were 1.7 and 0.34 mm respectively. Several accelerometers and pore pressure gauges were placed precisely at a depth of 4 cm and 10 cm from the ground surface. After filling the sand, the ground surface was carefully leveled by means of a vacuum, and then fully saturated by the percolation technique using Carbon dioxide gas and vacuum. The fluid used in this study was an aqueous solution of hydroxypropyl methylcellulose. The viscosity of fluid was controlled to be 25 m^2/s for the 25 G centrifuge model test by changing its concentrations.

Soon after reaching a centrifugal acceleration of 25 G, the model ground was subjected to seismic excitation of 50 sinusoidal waves with 4 Hz in the prototype scale. After confirming the dissipation of excess pore pressure generated in the previous excitation, the excitation level was increased stepwise until the model ground liquefied. A total of eleven model tests were carried out on the model ground prepared with various types of grid spacing by the PARI Centrifuge (Kitazume and Miyajima, 1995).

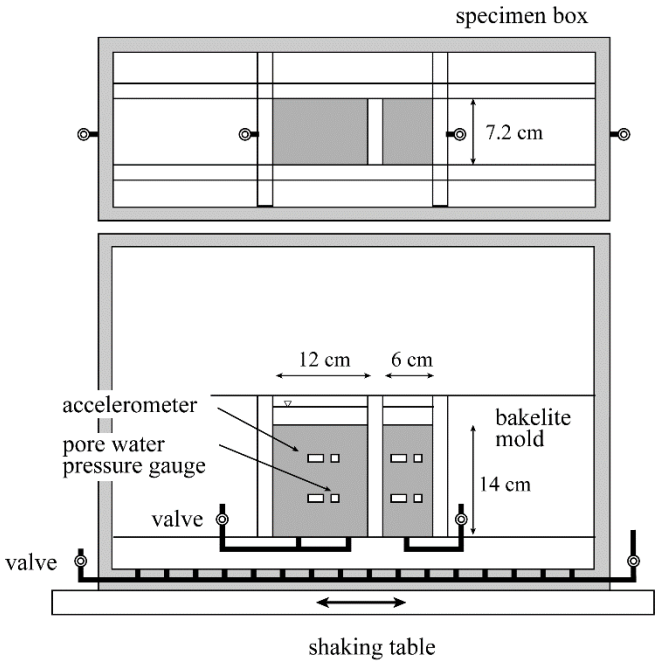

(a) Schematic view of model ground.

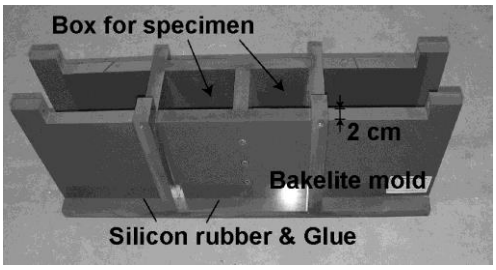

(b) Bakelite model panels.

Figure 15. Model ground (Takahashi *et al.*, 2006).

The relationships between the induced acceleration at a depth of 1.0 m (values are quoted in prototype scale in this subsection) and input excitation are plotted in Figure 16. The induced acceleration measured in various grid spacing initially increases almost linearly with increasing the input acceleration. The induced acceleration for the wall spacing, *L* of 2.0 m shows a sharp decrease at the input excitation of about 380 *gal*, which indicates that liquefaction took place in the ground. The model ground having the *L* of 1.5 m doesn't show sharp decreases in the acceleration even if the input acceleration exceeds about 500 *gal*. Similar phenomenon can be seen in the measurements at a depth of 2.5 m.

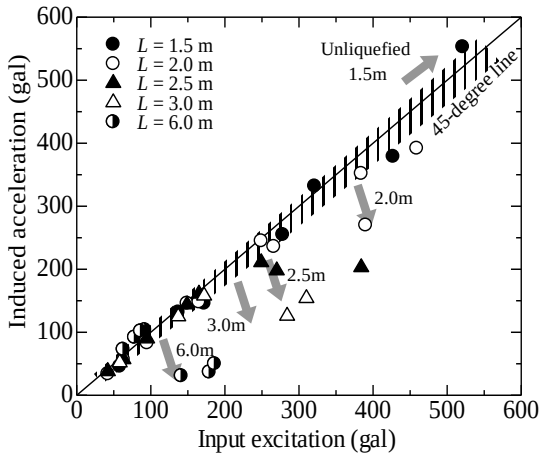

Figure 16. Relationship between induced acceleration and input excitation at a depth of 1.0 m (Takahashi *et al.*, 2006).

The relationship between the maximum excess pore pressure ratio, $\Delta u/\sigma'$ measured at depths of 1.0 m and 2.5 m and the input excitation is shown in Figure 17. For the depth of 1.0 m (Figure 17(a)), as the input excitation increases, the $\Delta u/\sigma'$ increases gradually irrespective of the grid spacing. The $\Delta u/\sigma'$ increases to unity in the case where *L* is equal to or exceeds 2.0 m, and the input acceleration at that time decreases as increasing the *L* value. In the ground with *L* of 1.5 m, the $\Delta u/\sigma'$ does not increase to unity even when the input acceleration exceeds about 500 *gal*. For the depth of 2.5 m (Figure 17(b)), as the input excitation increases, the $\Delta u/\sigma'$ increases gradually irrespective of the grid spacing. The $\Delta u/\sigma'$ increases to unity in the case where *L* is equal to 6.0 m. In the ground with *L* lower than 3.0 m, the $\Delta u/\sigma'$ does not increase to unity even when the input acceleration exceeds about 500 *gal*. According to the above discussion, the improvement effect on liquefaction prevention is highly influenced by the grid spacing.

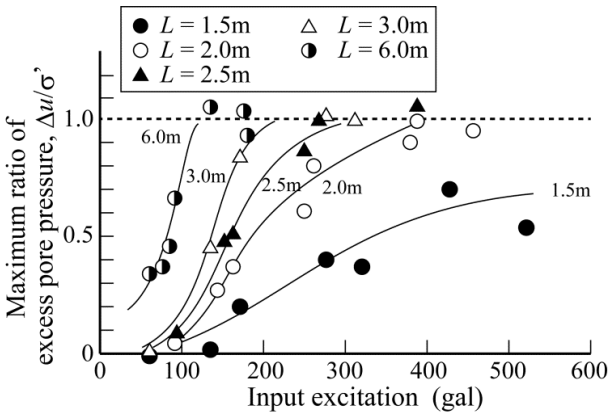

(a) G.L. -1.0m

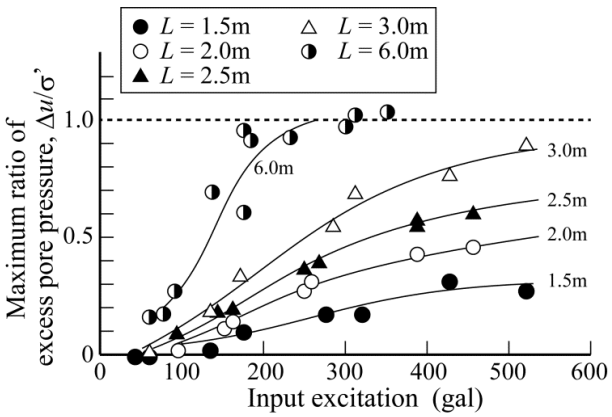

(b) G.L. -2.5m

Figure 17. Relationship between maximum ratio of excess pore pressure and input excitation (Takahashi *et al.*, 2006).

Figure 18 shows the relationship between the grid spacing to grid height ratio, *L/H* ratio and the excess pore water pressure ratio. The *d* in the figure is the concerned depth measured from the ground surface. In the case of *d/H* of 0.3, the pore water ratio increases to 1.0 at the *L/H* of about 0.9 and 0.7 for the small acceleration of 150 – 180 *gal.* and the large acceleration of 250 – 280 *gal*, respectively. In the case of *d/H* of 0.7, the pore water ratio increases to 1.0 at the *L/H* of about 3.0 and 2.0 for the small acceleration of 150 – 180 *gal* and the large acceleration of 250 – 280 *gal*, respectively. The test results indicates that the liquefaction can take place at the shallow portion by smaller acceleration than that at the deep portion.

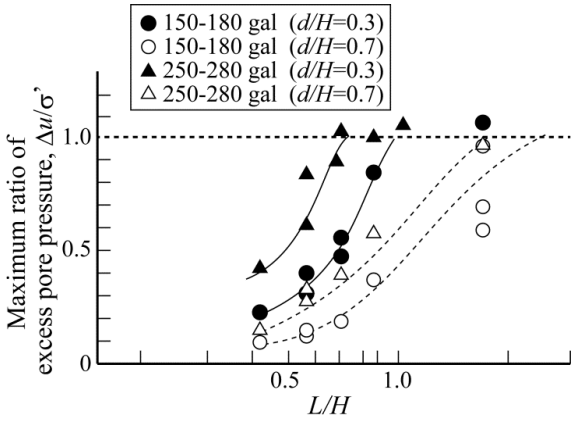

Figure 18. Relationship between maximum ratio of excess pore pressure and input excitation (Takahashi *et al*., 2006).

Figure 19 shows the relationship between the *L/d* ratio and the input acceleration. In the figure, the test data when liquefaction did or did not take place are plotted as a filled circle and an open circle, respectively. A gray-filled circle shows the excitation level where the ground liquefies to some extents during the figure. The boundary shows that the input acceleration necessary for liquefaction increases with de excitation. Based on the plotted data, a liquefaction boundary can be drawn as the hatched portion in the creasing *L/d*, very sharply when the *L/d* becomes less than about 2. This figure confirms that a large effect on liquefaction prevention can be expected when the *L/d* ratio becomes less than about 2. This figure also indicates that the liquefaction can be induced by a relatively small earthquake attack in the shallow depth of ground (i.e. having a small *d* value) even if the grid spacing is quite small. This suggests a limitation in the application of the grid type improvement for liquefaction prevention, and the shallow ground should be improved by the other technique.

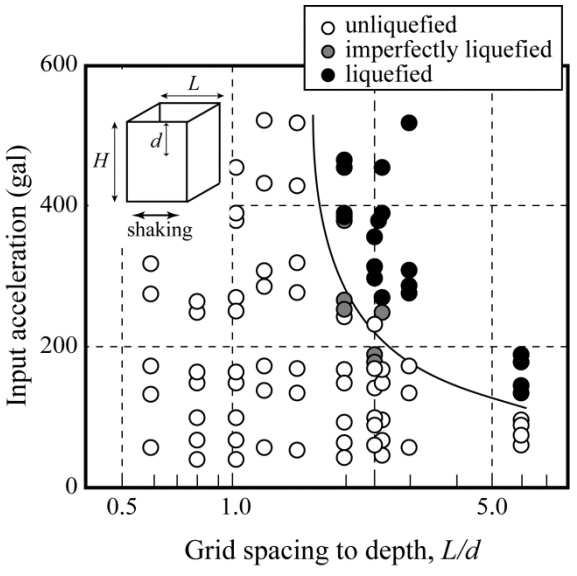

Figure 19. Relationship between input excitation and *L/d* (Takahashi *et al*., 2006).

Based on the accelerations and pore pressures measured in the model ground with five different grid spacing, it was confirmed that the improvement effect of liquefaction prevention was influenced by not only the grid spacing but also the magnitude of excitation and it also differs at different depth. A new parameter, the ratio of grid spacing to depth, *L/d*, was proposed to evaluate the effect of grid improvement on liquefaction prevention, as shown in Figure 19.

4.2 *Centrifuge test and numerical analyses on effect of grid space*

Architecture engineering research team of Takenaka Corp. also carried out a series of centrifuge model tests and FEM analyses to investigate the effect of the grid spacing for building foundation (Taya *et al*., 2008). Figure 20 shows the model ground, whose inside dimensions are 100 cm in length, 30 cm in width and 34.5 cm in thickness. They used a laminar box. Loose sand layer of Ooigawa sand with 70 % in

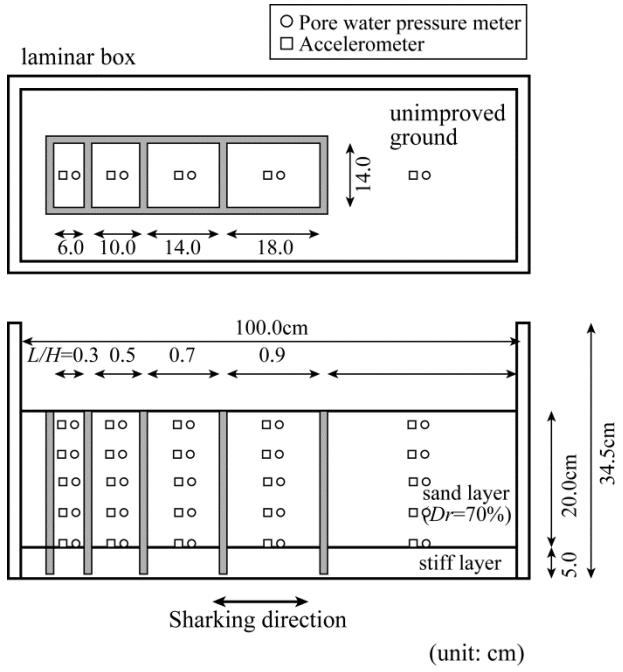

Figure 20. Model ground (Taya *et al*., 2008).

relative density was made on the stiff layer, and were saturated with silicone oil with 100 times large viscosity. The model ground was subjected to 20 cycle sinusoidal waves of 1.4 Hz at the centrifuge acceleration field of 100 *G*. The tests were carried out changing the depth of water table and the seismic intensity from around 80 to 260 cm/s^2.

Figure 21 shows the relationship between the grid spacing ratio, *L/H* and the maximum pore water pressure generation ratio, *Ru*. As far as the input acceleration remains small value, the *Ru* value increases with the increase of *L/H* ratio. However, the relationship is influenced by the magnitude of the input intensity and the water table depth.

The F_L value was calculated for the test condition by Eqs. (1) and (2), while the liquefaction resistance was calculated by Meyerhof's equation. Figure 22 shows the calculated F_L value and *Ru*, where the other centrifuge test data were also plotted together. The coefficients, *F(L)*, *F(G)* and *F(H)*, were derived as Eq. (3) by the numerical calculations incorporating the grid space, the stiffness of the grid and the improvement depth. Although there is a lot of scatter in the calculated data due to differences in the test conditions, the pore water pressure generation decreases sharply when the F_L value exceeds unity. The figure reveals the high applicability of the simple calculation, Eq. (2) for the design of grid spacing.

$$F_L = \left(\frac{\tau_1}{\sigma_z'}\right) \Big/ \left(\frac{\tau_d}{\sigma_z'}\right)_{\text{Grid}} \tag{1}$$

$$\frac{\tau_d}{\sigma_z'} = \gamma_n \cdot \frac{\alpha_{max}}{g} \cdot \frac{\sigma_z}{\sigma_z'} \cdot \gamma_d \cdot F(L) \cdot F(G) \cdot F(H) \tag{2}$$

$$\left.\begin{aligned} &\gamma_d = 1 - 0.033z \\ &F(L) = 0.287 \ln L - 0.095 \\ &F(G) = -0.459 \ln G + 4.026 \\ &F(H) = 0.689 \cdot e^{0.016H} \end{aligned}\right\} \tag{3}$$

where G = grid stiffness (MN/m^2); H = thickness of sand layer (m); L = grid space (m); z = depth (m); *F(L)* = coefficient for grid space; *F(G)* = coefficient for grid stiffness; and *F(H)* = coefficient for thickness of sand layer

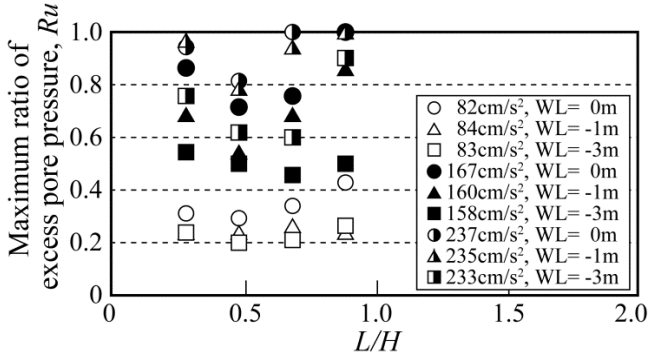

Figure 21. Relationship between *Ru* and *L/H* (Taya *et al.*, 2008).

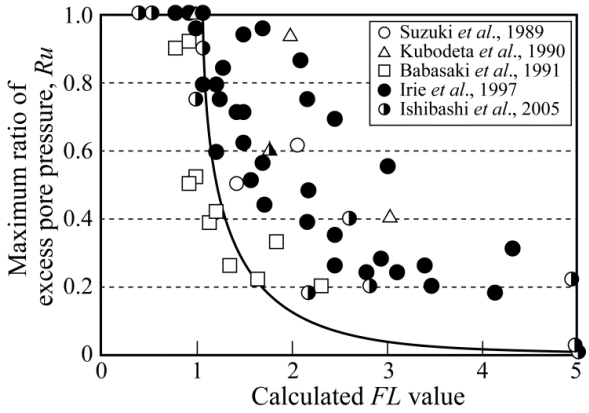

Figure 22. Relationship between *Ru* and F_L (Taya *et al.*, 2008).

Base on the centrifuge model tests and numerical simulations, they proposed a formulation as Eqs. (1) and (2) to evaluate the seismic shear stress of loose sand in the grid for building construction. The new design procedure has been adopted to many building construction projects and to evaluate the grid space more precisely.

4.3 *Application of the grid type DMM for embankment*

Yodo River flows from Lake Biwa to Osaka Bay through Osaka City. Due to the Hyogoken-Nambu Earthquake in January 1995, the river dike was heavily damaged for the length of 1.8 km because of slope failure due to ground liquefaction (Kamon, 1996). A representative cross section of the damaged dike is shown in Figure 23(a). The top portion of the river dike sank down about 3 m. The damaged dike had to be restored very quickly, because there was a risk of flooding during the rainy season which usually commenced in June. The ground condition at the site is shown in Figure 23(b). The ground consisted of a sandy layer and a clay layer. As the SPT *N*-value of the sandy layer was smaller than 10, the liquefaction might take place again in earthquake attack in the future.

Because there were many residential houses in the neighborhood along the river dike, it was necessary to avoid noise and vibratory problems during the construction. This was one of the reasons why the deep mixing method was applied there. The cross section of the improved ground is shown in Figure 23(c), where grid type improvement was applied to prevent the liquefaction of the ground and to improve the stability of river embankment. The grid of the stabilized soil columns was about 5 m by 5.4 m. The design strength of the stabilized column, q_u was 500 kN/m^2. Assuming the strength ratio of the field stabilized soil and laboratory stabilized soil, q_{uf}/q_{ul} was assumed 0.25 in the design, 90 or 100 kg/m^3 of blast furnace slag cement type B were mixed to achieve

the design strength for the sandy layer and clay layer respectively.

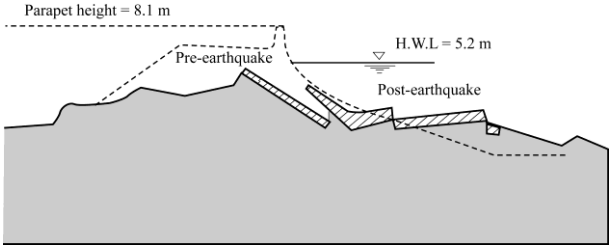

(a) Cross section of the Yodo River dike after the 1995 Hyogoken-Nambu Earthquake.

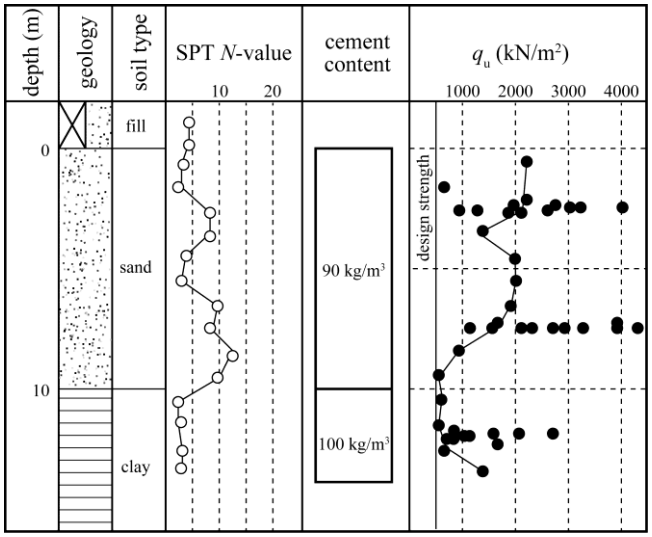

(b) Ground condition at the site.

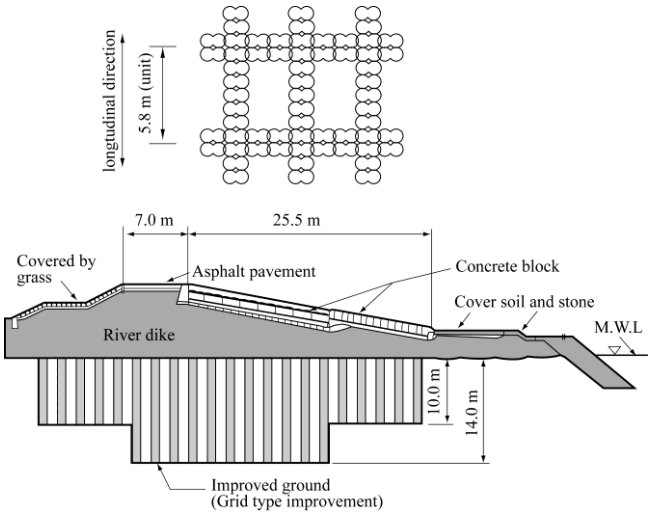

(c) Sectional view of DM improved ground.

Figure 23. Application of grid type deep mixing at the Yodo River dike.

4.4 *Application of the grid type DMM for building foundation*

Figure 24 shows an example of the application of the simple design to the building foundation. The superstructure of the building is a four-story parking facility, which was constructed in Urayasu-city, Chiba in 2006 (Uchida *et al*., 2012; 2013; 2014). In plan, the superstructure is rectangular with 213 m in length and 71 m in width. The mean dead load of the building on the ground surface is about 45 kN/m^2.

Figure 24(b) shows the ground condition. Landfill and a sand layer are distributed over the ground from the surface to a depth GL-14~16 m, and a soft clay layer is distributed over the lower part. The bottom depth of the clay layer changes greatly in the site, where the bearing stratum with SPT-N value over 50 appears at GL-39 m and at GL-72 m at the line 1 and line 20 of the building, respectively. SPT-N values of the landfill and sand layer from the surface to around GL-14 m are around 10. The water table is at GL-1.8 m. Figure 24(c) indicates the liquefaction potential of the site according to Architectural Institute of Japan recommendations for foundations (AIJ, 2001). When the surface acceleration on the site is estimated at 200 cm/s^2, the liquefaction potential, F_L becomes less than 1.0 in the depth from GL-1.8 m to GL-12 m. This result suggests that the liquefaction is likely to occur in this site during a large earthquake. Therefore, to prevent liquefaction of the landfill and sand layer on the site, the grid-form ground improvement method was selected to insure a good performance of the piled-raft foundation adopted for the building. To decrease settlement of the superstructure, prestressed high-strength concrete (PHC) piles with diameters from 500 mm to 1000 mm and lengths from 33 m to 60 m were used. The length of piles and soil improvement were selected based on data of 13 soil borings on the site.

The typical 15.6 m by 16.5 m grid-form ground improvement was adopted for the building. The specifications of the grid-form ground improvement were decided based on the AIJ recommendations for ground improvement (Architectural Institute of Japan, 2006) and the simplified method proposed by Taya *et al*. (2008). The unconfined compressive strength of the improved soil assumed for design was 1.8 MN/m^2. Ground improvement was performed by using the two-axle type mixing machine. After completion of the ground improvement, improved soil samples were recovered and tested. The unconfined compressive strength of these samples after cured for four weeks was in the range 3.3 - 9.8 MN/m^2 (with an average value of 5.8 MN/m^2).

The building and the improved ground were subjected to the large earthquake in 2011. Extensive soil liquefaction was observed in the reclaimed land of Urayasu city, where sand boils were confirmed

around the site. Figure 24(a) shows the building condition just after the earthquake (photo taken on March 13, 2011). While small settlement was confirmed in the ground side 3 to 4 m away from the building, no ground damage such as sand boils were observed during the field investigation around the building.

(a) Building on grid type deep mixing improved ground.

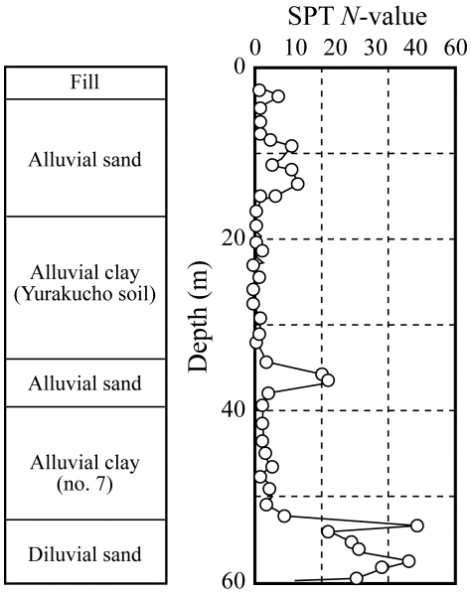

(b) Ground condition at the site (Boring No. 2).

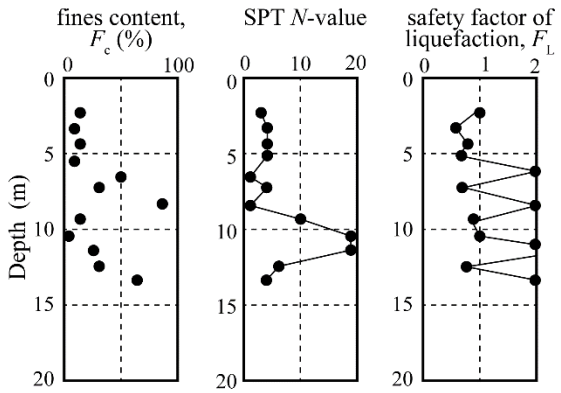

(c) Liquefaction potential at the site (Boring No. 6).

Figure 24. Application of grid type deep mixing improved ground (Uchida *et al.*, 2012).

4.5 *Other Applications of the grid type DMM*

Soon after the aftermath of the 2011 Tohoku earthquake and tsunami, the Cement Deep Mixing Association, the Dry Jet Mixing Association and Chemical Grouting Co. Ltd. conducted field surveys in the Tohoku and Kanto areas to investigate any deformation and damage in the deep mixing improved ground and the performance of the improved grounds. Though few slight deformations were found in some grounds, as a whole no serious deformation and damage was found in the improved ground and superstructures even they were subjected to quite large seismic force (Kitazume, 2012). Here, two applications in the field surveys are briefly introduced.

4.5.1 *Road embankment*

The road embankment at Soga, Chiba Prefecture, was improved by the grid type deep mixing method for liquefaction prevention. The original ground beneath the embankment contains large amount of fine sand to the depth of -7 m, which was anticipated to be highly liquefied due to earthquake motion. The improved ground has about 5.6 m in width, 6.0 m in height, and the improvement area ratio of 50%, and whose unconfined compressive strength, q_u is 200 kN/m^2 (Figure 25(a)). No damage was found in the embankment and the improved ground as shown in

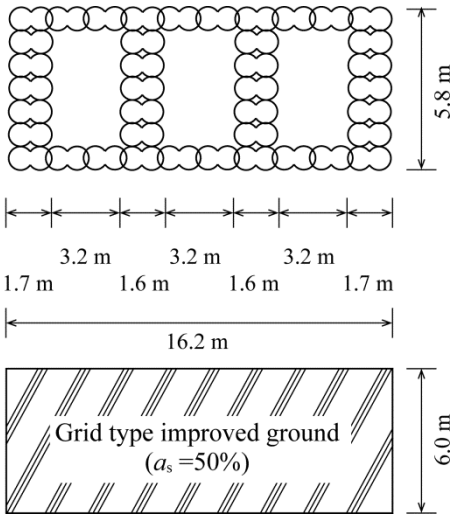

(a) Layout of ground improvement.

(b) Road at improved are after earthquake.

(c) Road at unimproved area after earthquake.

Figure 25. CDM improved ground at Soga, Chiba Prefecture,.

Figure 25(b), even subjected to the seismic force of 5.0 upper in Japanese Magnitude-Shindo (seismic intensity scale). As contrast, Figure 25(c) shows heavy damage of road without improvement located in the neighborhood due to liquefaction.

4.5.2 *River embankment*

The foundation for the river embankment in Chiba Prefecture was improved by the grid type DM method as shown in Figure 26(a), where the width and height of the improved ground were 21.0 m and 21.0 m respectively. The improvement area ratio and the design strength were 50.6% and the de sign unconfined compressive strength, q_{uck} of 600 kN/m^2 respectively. No damage was found in the embankment and the improved ground, as shown in Figure 26(b).

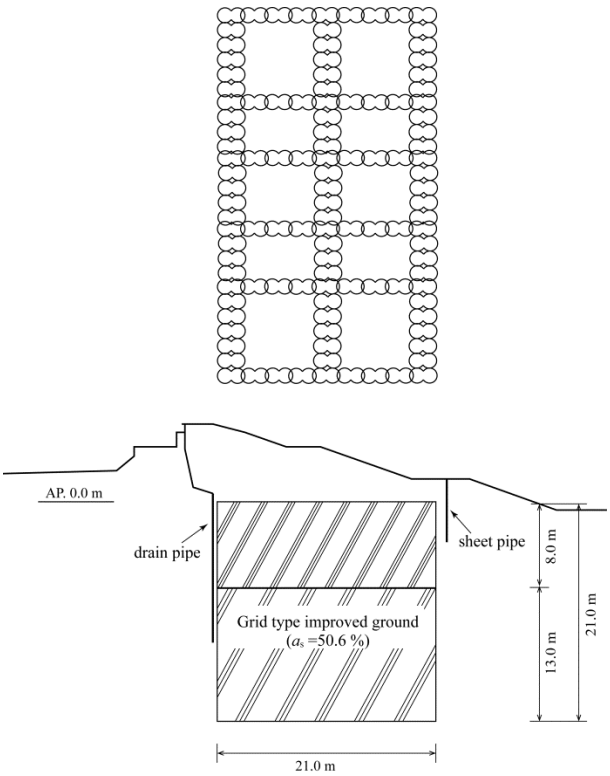

(a) Layout of ground improvement.

(b) River embankment after earthquake.

Figure 26. DJM improved ground for the river embankment in Chiba Prefecture.

5. DEVELOPMENT OF FLOATING TYPE IMPROVEMENT

5.1 *Centrifuge model test*

According to the previous researches, it is well known that liquefaction can take place at shallow layer than deep layer, which indicates the grid space can be increased at deep layer. In order to promote more economical and reasonable design of the grid, a series of centrifuge model tests was carried out on the floating type improved ground (Takahashi *et al.*, 2006; 2012a; 2012b). In the tests, two types of model ground were prepared and subjected to seismic loading in the 50 *G*.

Figure 27 shows the model ground, the center grid is shallower than the outer grid. The model grid was made of Bakelite panels with the thickness of 2 cm. The model grid was fixed on the specimen box with bolts. Several model grids were prepared to perform parametric tests. The center grid was made by aluminum plate which could be changed the depth of 4, 7 and 10 cm. The sand material used in this study was Soma sand, whose U_c and D_{10} were 1.7 and 0.34 mm respectively. Several accelerometers and pore pressure gauges were placed precisely at a depth of 4 cm and 10 cm from the ground surface. The sand layer was fully saturated by the percolation technique using Carbon dioxide gas and vacuum. The fluid used in this study was an aqueous solution of hydroxypropyl methylcellulose. The viscosity of fluid was controlled to be 25 m^2/s for the 25 *G* centrifuge model test by changing its concentrations.

Soon after reaching a centrifugal acceleration of 25 *G*, the model ground was subjected to seismic excitation of 50 sinusoidal waves with 4 Hz in the prototype scale. After confirming the dissipation of excess pore pressure generated in the previous excitation, the excitation level was increased stepwise until the model ground liquefied. A total of eleven model tests were carried out on the model ground prepared with various types of grid spacing.

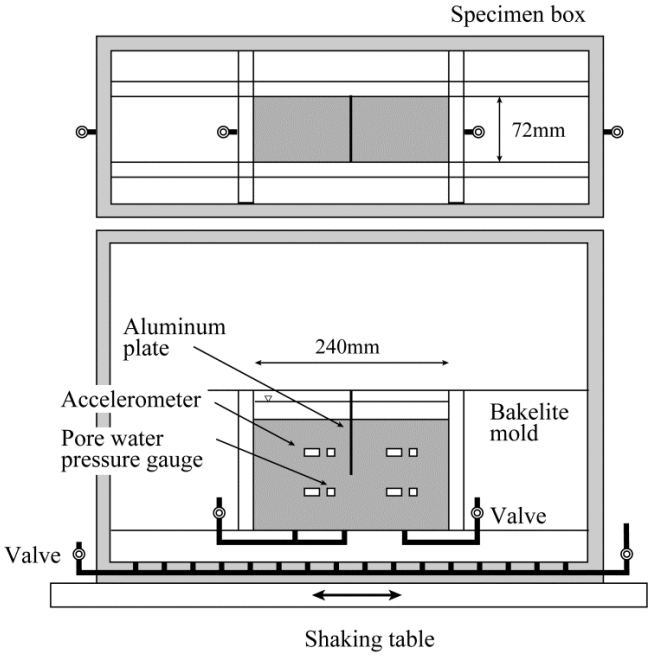

Figure 27. Schematic view of model ground (Takahashi *et al*., 2006).

Figure 28 shows the relationship between the seismic acceleration and the pore water pressure ratio, $\Delta u/\sigma'$. At the depth of 1.0 m (Figure 28(a)), the pore water pressure ratio increases at the acceleration of 60 *gal*, and increases to 1.0 at the acceleration of 100 *gal* in the no center grid case. In the case of the center grid depth is 3.0 m (reaches to the bottom) and 2.5 m, the pore water pressure ratio increases at the acceleration of 70 *gal*, and reaches to 1.0 at the acceleration of 170 *gal*. At the depth of 1.75 m (Figure 28(b)), the pore water pressure generates very fast in the case of the center grid depth is 0 (no grid), 1.0 and 1.75 m. In the case of 3.0 m depth (reaches to the bottom), the pore water pressure ratio increases slowly to 1.0 at the acceleration of 400 *gal*. At the depth of 2.5 m (Figure 28(c)), the pore water pressure generates with the input excitation, but the ratio reaches to 1.0 at the larger acceleration than that for shallow depth.

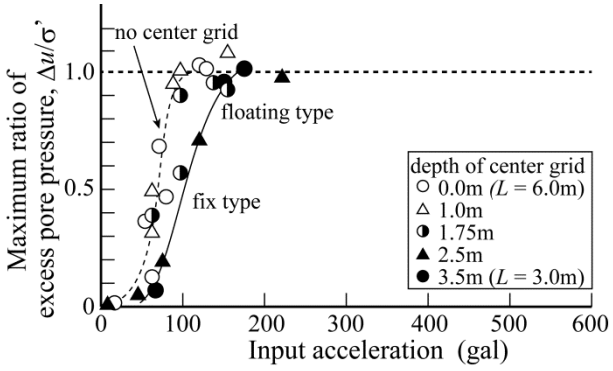

(a) at depth of 1.0 m.

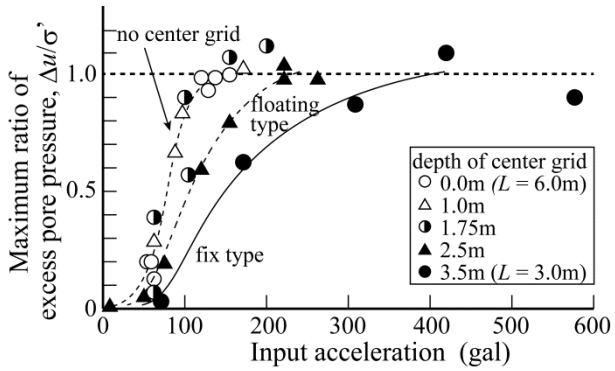

(b) at depth of 1.75 m.

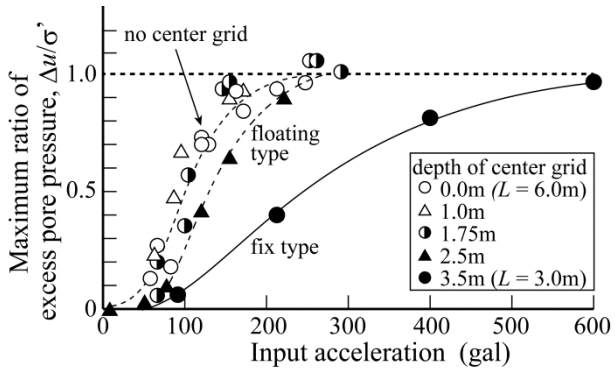

(c) at depth of 2.5 m.

Figure 28. Relationship between the seismic acceleration and the pore water pressure ratio, $\Delta u/\sigma'$ (Takahashi *et al*., 2006).

Figure 29 shows the relationship between the improvement depth and the seismic acceleration when liquefaction takes place. Figure 29(a) and 29(b) show the grid width of 6.0 m and 3.0 m, which corresponds the no center grid case and the fixed type grid cases respectively. Figure 29(c) to 29(e) shows the test cases at various depths of the center grid. In the figure, black circle and white circles indicate the liquefaction takes place and no liquefaction takes place respectively. Figure 29(a) and 29(b) shows that the seismic acceleration at liquefaction taking place increases with the depth, and the acceleration at liquefaction is smaller in the case of the grid space of 3.0 m rather than that of 6.0 m. Figure 29(c) shows similar behavior of the grid space of 6.0 m (Figure 29(b)), which means that negligible effect of the center grid to liquefaction prevention. In the case of the depth of the center grid of 1.75 m, Figure 28(d), the seismic acceleration at the depth of 1.0 m becomes larger. In the case of the depth of the center grid of 2.5 m, Figure 28(d), the seismic acceleration at liquefaction at the depth of 1.0 m is almost same as that of the grid space of 3.0 m (Figure 28(a)). The test results shows that almost same liquefaction prevention effect can be expected even the depth of the center grid reduced. This is large benefits for the ground where liquefiable layer is large thickness.

Based on the research results, the technical manual on the floating and grid type improved ground was

proposed for further application (Coastal Development Institute of Technology, 2014).

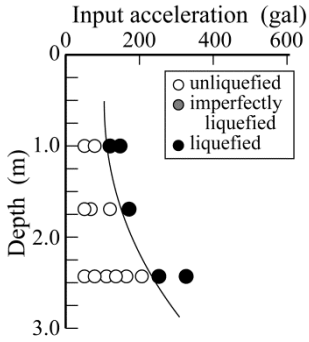

(a) grid space of 6.0 m

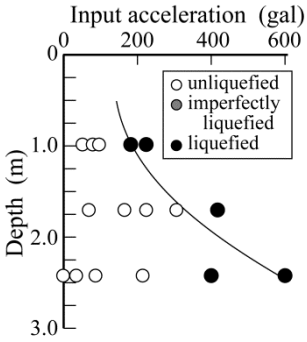

(b) grid space of 3.0 m.

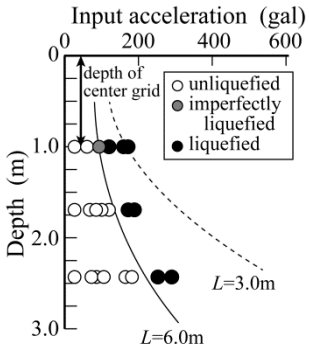

(c) grid depth of 1.0 m

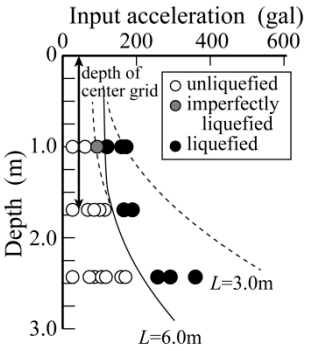

(b) grid depth of 1.75 m.

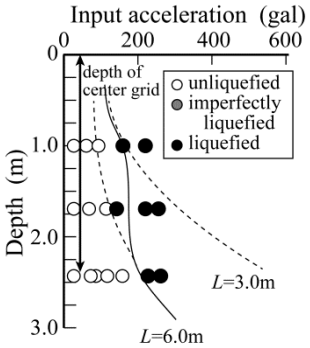

(d) grid depth of 2.5 m

Figure 29. Relationship between the seismic acceleration and the pore water pressure ratio, $\Delta u/\sigma'$ (Takahashi *et al.*, 2006).

6. CONCLUDING REMARKS

This manuscript emphasizes the importance of liquefaction mitigation to minimize earthquake disaster. Then it briefly describes the introduction and development history of the grid type deep mixing method for liquefaction mitigation together with the application and contribution of the centrifuge model testing for the method. The grid type deep mixing has been often applied to many types of infrastructures and many building foundations, and its high applicability and improvement effect have been evaluated in many earthquakes. Its design, execution and quality control and assurance have been improved based on the accumulated laboratory and field experiments, numerical analyses, field experiences and know-how.

Many centrifuge model tests on the grid type deep mixing were carried out to investigate the effect of grid space, the external and internal stabilities of the improved ground. In many tests on the effect of grid space, a quite simple model ground with Bakelite grid walls were adopted, and several grids with various size were tested in one test for parametric study. However, the best acre was paid in the centrifuge model tests for density control and saturation of ground so that the interaction of the soil layer and the grid wall could be obtained precisely. The high quality model tests could provide very large contributions to the development of the method.

Since the 2011 Tōhoku earthquake, the necessity and importance of earthquake reinforcement and liquefaction mitigation have been highlighted on new infrastructures and existing residential houses. Especially in Urayasu city, the liquefaction countermeasure will be conducted to more than a thousand of residential houses by the grid type deep mixing, as they were damaged by liquefaction. A large number of the numerical analyses and centrifuge tests were performed for the detail design of each house. The detail of the design together with centrifuge tests and numerical analyses will be presented in future.

REFERENCES

Architectural Institute of Japan. 2006. *Seismic response analysis and design of buildings considering dynamic soil-structure interaction* (in Japanese).

Babasaki, R., Suzuki, K. and Suzuki, Y. 1992. Centrifuge tests on improved ground for liquefaction, *Proc. of the 10th World Conference on Earthquake Engineering*: 1461-1464.

Babasaki, R., Suzuki, K., Suzuki, Y. & Fujii, N. 1991. Cell type foundation improved by deep cement mixing method against soil liquefaction (Part 2) Centrifugal vibratory tests on cell type foundation, *Proc. of the 26th Annual Conference on Soil Mechanics and Foundation Engineering*: 1007-1008 (in Japanese).

Coastal Development Institute of Technology. 2014. *Technical Manual of Floating and Grid Type Deep Mixing Method* (in Japanese).

Fujii, N., Kusakabe, O., Keto, H. & Maeda, Y. 1988. Bearing capacity of a footing with an uneven base on slope: Direct comparison of prototype and centrifuge model behavior, *Proc. of the Centrifuge 88*: 301-306.

Inatomi, T., Uwabe, T., Iai, S., Tanaka, S., Yamazaki, H., Miyai, S., Nozu, A., Miyata, M. & Fujimoto, Y. 1997. Damage to port structure by the 1994 East Off Hokkaido Earthquake. *Technical Note of the Port and Harbour Research Institute*, 856: 1-583 (in Japanese).

Kamon, M. 1996. Effect of grouting and DMM on big construction projects in Japan and the 1995 Hyogoken-Nammbu earthquake. *Proc. of the 2nd International Conference on Ground Improvement Geosystems*. 2: 807-823.

Kazama, M., Inatomi, T. & Imamura, T. 1983. Observation and analysis of seismic response of grid type improved ground

by deep mixing method, *Report of the Port and Harbour Research Institute*, 22(4): 141-180 (in Japanese).

Kitazume, M. 2012. Soil mixing performance in the 2011 Tohoku earthquake, *The Magazine of the Deep Foundations Institute*:77-78.

Kitazume, M. & Miyajima, S. 1995. Development of PHRI Mark II geotechnical centrifuge, *Technical Note of the Report of the Port and Harbour Research Institute*, 817: 1-33.

Kitazume, M. 2009. Twenty Nine Years of experiences of physical modeling of geotechnical problems in port structures, *International Journal of Physical Modelling in Geotechnics* 9(3): 1-19.

Kitazume, M. & Terashi, M. 2013. *The Deep Mixing Method*: CRC Press, Taylor & Francis Group.

Koga, Y., Taniguchi, E., Nakasumi, I. & Kurinami, K. 1986. Shaking table tests on DMM method as a countermeasure against liquefaction of sandy ground, *Proc. of the 41st Annual Conference on Japan Society of Civil Engineers*: 201-202 (in Japanese).

Koga, Y., Matsuo, O., Enokida, M., Ito, K. & Suzuki, K. 1988. Shaking table tests on DMM method as a countermeasure against liquefaction of sandy ground (Part 2) Effects of improved ground in grid configuration against liquefaction, *Proc. of the 23th Annual Conference on Soil Mechanics and Foundation Engineering*: 1019-1020 (in Japanese).

Koseki, J., Kubodera, I., Ito, K., Suzuki, K., Nishioka, S. & Fukada, H. 1991. Study of the applicability of deep mixing method as a countermeasure system against liquefaction – Numerical analysis by means of DIANA-J, *Proc. of the 26th Annual Conference on Soil Mechanics and Foundation Engineering*: 1015-1016 (in Japanese).

Matsuo, O., Koseki, J., Fukada, H., Kubodera, I., Suzuki, K. & Nishioka, S. 1991a. Shaking table tests on DMM method as a countermeasure against liquefaction of sandy ground (Part 3) Effects of improved ground in grid configuration against liquefaction, *Proc. of the 26th Annual Conference on Soil Mechanics and Foundation Engineering*: 1009-1010 (in Japanese).

Matsuo, O., Koseki, J., Suzuki, K., Nishioka, S., Fukada, H. & Kubodera, I. 1991b. Shaking table tests on DMM method as a countermeasure against liquefaction of sandy ground (Part 4) External loads acting on the DMM improved soil part, *Proc. of the 26th Annual Conference on Soil Mechanics and Foundation Engineering*: 1013-1014 (in Japanese).

Matsuo, O. & Shimizu, T. 1994. Experimental study of design procedures for the deep mixing method used as a liquefaction prevention measure in embankments, *Civil Engineering Journal*: 36(7) (in Japanese).

Matsuo, O., Shimizu, T., Goto, Y., Suzuki, Y., Okumura, R. & Kuwabara, M. 1996. Deep mixing method as a liquefaction prevention measure, *Proc. of the 2nd International Conference on Ground Improvement Geosystems, IS-TOKYO'96*: 521-526.

Ministry of Construction. 1999. Design and construction manual of liquefaction prevention techniques (draft), *Joint Research Report*: 186 (in Japanese).

Ministry of Land, Infrastructure, Transport & Tourism. 2007. *Technical Standards for Port and Harbour Facilities* (in Japanese).

Namikawa, T., Koseki, J. & Suzuki, Y., 2007. Finite element analysis of lattice-shaped ground improvement by cement-mixing for liquefaction mitigation, *Soils and Foundations*, 47(3): 559-576.

Namikawa, T., Suzuki, Y. & Koseki, J. 2005. Seismic response analysis of lattice-shaped ground improvements, *Proc. of the International Conference on Deep Mixing, Best Practice and Recent Advances*, (1.2): 263-271.

Noda, S. 1991. Waterfront development and liquefaction, *Journal of the Japanese Society of Soil Mechanics and Foundation Engineering, 'Tsuchi-to-Kiso'*, 39(2): 1-4 (in Japanese).

Suzuki, K., Babasaki, R. & Suzuki, Y. 1991. Centrifuge Tests on liquefaction-proof foundation, *Proc. of the Centrifuge 91'*: 1461-1464.

Suzuki, K., Babasaki, R., Suzuki, Y. & Fujii, N. 1990. Cell type foundation improved by deep cement mixing method against soil liquefaction (Part 1) Centrifugal vibratory tests by a laminar box, *Proc. of the 25th Annual Conference on Soil Mechanics and Foundation Engineering*: 1035-1036 (in Japanese).

Suzuki, Y., Saitoh, S., Onimaru, S., Kimura, G., Uchida, A. & Okumura, R. 1996. Grid-shaped stabilized ground improved by deep cement mixing method against liquefaction for a building foundation, *Journal of the Japanese Society of Soil Mechanics and Foundation Engineering, 'Tsuchi-to-Kiso'*, 44(3): 46-48 (in Japanese).

Takahashi, H. & Hayano, K. 2009. Dynamic model tests in centrifuge on lattice-shaped DMM ground improvement for restraining displacement of quay wall, *Proc. of the International Conference on Performance-based Design in Earthquake geotechnical Engineering, IS-Tokyo 2009*, .

Takahashi, H. Morikawa, Y., Tsukuni, S., Fukutake, K., Suzuki, W. and Takehana, K. 2012a. Experimental study on floating lattice-shaped cement treatment method applied to liquefiable ground, *Journal of Japan Society of Civil Engineer*s, 68(2): I_432-I_437 (in Japanese).

Takahashi, H., Morikawa, Y., Tsukuni, S., Yoshida, M. & Fukada, H. 2012b. Approach to reducing improvement depth of lattice-shaped cement treatment method for liquefaction countermeasure, *Report of Port and Airport Research Institute*, 51(2): 3-39 (in Japanese).

Takahashi, H., Yamawaki, S., Kitazume, M. & Ishibashi, S. 2006. Effects of DMM on liquefaction prevention and proposal on new arrangement of grid-type improvement, *Report of Port and Airport Research Institute*, 45(2): 135-167 (in Japanese).

Taya, Y., Uchida, A., Yoshizawa, M., Onimaru, S., Yamashita, K. & Tsukuni, S. 2008. Simple method for determining lattice intervals in grid-form ground improvement, *Electrical Journal of Geotechnical Engineering*, 3(3): 203-212 (in Japanese).

Tokimatsu, K., Mizuno, H. & Kakurai, M. 1996. Building damage associated with geotechnical problems, *Soils and Foundations*, Special Issue 1: 219-234.

Uchida, A., Odajima, N. & Yamashita, K. 2013. Performance of building foundation with grid-form ground improvement during the 2011 Tohoku pacific earthquake, *Architectural Institute of Japan Journal of Technology*, 19(42):481-484 (in Japanese).

Uchida, A., Tsukuni, S., Akashi, T., Ohashi, M. & Arai, H. 2014. Simplified evaluation method about effect of liquefaction countermeasure for the grid-form deep mixing walls, *Architectural Institute of Japan Journal of Technology*, 20(46):921-924 (in Japanese).

Uchida, A., Yamada, T. Odajima, N. & Yamashita, K. 2012. Piled raft foundation with grid-form ground improvement subjected to the 2011 earthquake, *Proc. of the 9th International Conference on Urban Earthquake Engineering/4th Asian Conference on Earthquake Engineering*: 151-156.

Washida, S., Koga, Y., Koseki, J., Horii, K. & Nishihara, S. 1993. Enclosure method by sheet piling for the embankment of liquefiable ground, *Proc. of the 28th Annual Conference of the Japanese Society of Soil Mechanics and Foundation Engineering*: 2483-2486 (in Japanese).

Yamazaki, H. 2000. Current and trend of ground improvement techniques for liquefaction prevention for port facilities (2) -

Effectiveness and trend of techniques -. *Japan Society of Civil Engineers Magazine, Civil Engineering*. 85: 60-62 (in Japanese).

Zen, K., Yamazaki, H., Watanabe, A., Yoshizawa, H. & Tamai, A. 1987. Study on a reclamation method with cement-mixed sandy soils - Fundamental characteristics of treated soils and model tests on the mixing and reclamation. *Technical Note of the Port and Harbour Research Institute*, 579: 1-41 (in Japanese).